Infrared Physics & Technology 76 (2016) 393–401

Contents lists available at ScienceDirect

Infrared Physics & Technology

journal homepage: www.elsevier.com/locate/infrared

Regular article

# Evaluation of paint coating thickness variations based on pulsed Infrared thermography laser technique

S. Mezghani [a,*], E. Perrin [a], V. Vrabie [a], J.L. Bodnar [b], J. Marthe [c], B. Cauwe [c]

[a] CReSTIC/Châlons, Université de Reims Champagne-Ardenne, Chaussée du port, 51000 Châlons-en-Champagne, France
[b] GRESPI/ECATHERM, Université de Reims Champagne-Ardenne, BP 1039, 51687 Reims, France
[c] CRITT-MDTS, 3 Boulevard Jean Delautre – ZHT du Moulin Leblanc, 08000 Charleville-Mézières, France

## HIGHLIGHTS

- The Laser Infrared Thermography is an accurate non-destructive tool to evaluate the heterogeneity of paint coatings thickness.
- Two characteristic parameters were defined from the thermal response of coated sample.
- The investigations were conducted on a wide range of paint coating thickness variations.
- Numerical simulations were performed in order to optimize the parameters of excitation and analyze their behavior.
- Evaluation of the paint coating thickness on real sample shows a good accuracy in agreement with Eddy current methods.

## ARTICLE INFO

*Article history:*
Received 12 October 2015
Revised 27 March 2016
Accepted 28 March 2016
Available online 30 March 2016

*Keywords:*
Non-destructive evaluation
Coating thickness variations
Heterogeneity
Pulsed Infrared thermography
Laser heating

## ABSTRACT

In this paper, a pulsed Infrared thermography technique using a homogeneous heat provided by a laser source is used for the non-destructive evaluation of paint coating thickness variations. Firstly, numerical simulations of the thermal response of a paint coated sample are performed. By analyzing the thermal responses as a function of thermal properties and thickness of both coating and substrate layers, optimal excitation parameters of the heating source are determined. Two characteristic parameters were studied with respect to the paint coating layer thickness variations. Results obtained using an experimental test bench based on the pulsed Infrared thermography laser technique are compared with those given by a classical Eddy current technique for paint coating variations from 5 to 130 μm. These results demonstrate the efficiency of this approach and suggest that the pulsed Infrared thermography technique presents good perspectives to characterize the heterogeneity of paint coating on large scale samples with other heating sources.



## 1. Introduction

Coating technology is widely used in various industries and applications to achieve functional surfaces such as wear resistance, corrosion resistance, and cosmetic aspect [1]. The coating thickness needs to be controlled and mastered because it has a great influence on the final product performance (weight, friction, corrosion, aspect, etc.) [2]. Commercially available thickness meters, including cross-section microscopy or gravimetric (mass) measurement [3], might be destructive by inducing surface damage and are limited in spatial sampling resolution. These methods are used when non-destructive methods are not possible, or as a way of confirming non-destructive results.

Non-destructive measuring techniques are also used for coating thickness evaluation. *Magnetic gauges* [4,5] are based on magnetic flux measurement through the layer of sample. The inadequacy of this method is the determination of thickness for multilayered coating layer. *Eddy current methods* [6] use the interaction between a magnetic field source (i.e. coil probe) and the testing material to determine the thickness of the coating. It's a comparative measure between the signal collected from sample and the reference one [7]. However, this method can be used only on conductive materials and sensitivity decreases with depth depending on the conductivity and permeability of the substrate. *Ultrasound testing*, which can be used to estimate the paint thickness on nonmetal substrates, is based on the control of the velocity of ultrasonic waves in the coating layer [8]. The ultrasonic sensor may be combined with other method such as Eddy current [9] or capacitance sensors. The ultrasound testing requires a coupling medium to transfer the

* Corresponding author.
*E-mail address:* sihem.mezghani@univ-reims.fr (S. Mezghani).

http://dx.doi.org/10.1016/j.infrared.2016.03.018
1350-4495/

energy into the test specimen and materials that are irregular in shape. Very thin or not homogeneous coatings are difficult to inspect, this technique not being well adapted on the measurement of heterogeneities. *Terahertz methods* measure the time delay of a terahertz waveform using different analyzing techniques such as terahertz imaging [10], terahertz sensor [11] or time-domain spectroscopy [12], but they require the knowledge of the refractive index of each layer of the sample for calculating the coating thickness. To enhance the thickness measurement, pattern-based partial least squares were applied following the terahertz process [13]. It has made it possible to formulate a calibration function for coating thickness estimation, but this prediction procedure is well adapted for a thickness of less than 10 μm [13].

The choice among these measurement methods depends on the coating thickness, the cost of instrumentation and the accuracy required [14]. The infrared thermography technique is an interesting alternative nondestructive evaluation method. The test material is excited by a flow of heat, resulting in a change in local thermal conditions. The thermal variations of the material to this excitation is captured by a thermal infrared camera. The acquired thermal response depends on different parameters of the material such as thermal conductivity, diffusivity, emissivity, and specific heat as well as the excitation used at the input [15]. More specifically, the above properties manifest themselves in the thermal response depending upon different factors including the coating heterogeneities. Infrared thermography based measurement is considered as an interesting non-destructive technique for material inspection in various applications such as civil structures [16–18], evaluation of fatigue damages in materials [19–21], aerospace [22,23], and automotive [24]. Thermal imaging presents several benefits: remote sensing, two-dimensional data acquisition, rapid response, non-contact, high resolution, large temperature range, post-processing versatility and portability [25].

Given the potential for relative simplicity, low weight compact and inexpensive nature of temperature-based measurements using thermal camera, non-destructive evaluation of painting and coating can be done by the infrared thermography technique [14]. This technique might be potentially used to evaluate the heterogeneity of the coating for an entire sample [26]. In such applications, a flash heating excitation was proposed by Aoyagi et al. [14]. However, it has been shown that this method allows to detect uneven painting only when the variations in thickness are roughly of the order of 20 μm. Evaluating the heterogeneity of large surfaces is not a simple task since the temperature variations of coated samples are dependent not only on the substrate and paint properties, but also on the thermal properties of the paint and the geometry of the acquisition system. Other signal processing algorithms such as Markov-PCA [27] has been proposed for characterization of depth variation in presence of deboned defect on carbon fiber reinforced composites. This technique improves the signal-to-noise (SNR) of feature images in pulsed phase thermography, but the question still remains: can the infrared thermography take advantage of specific nature of the thermal signal to have a good estimation of coating thickness variations?

In this paper, we propose to analyze the capacity of the infrared thermography technique to assess the thickness variations of paint coatings. A numerical simulation model using a finite element model in COMSOL Multiphysics software and supposing uniform and isotropic coatings has been firstly used. This model is useful for analyzing the behavior of the characteristic parameters that can be extracted from the thermal responses to variations of the paint coating and substrate. Such analysis allows us to identify the optimal experimental parameters that better differentiate only the variations of the paint coating. Next, an experimental test bench using a pulsed laser source and an Infrared thermal camera was used to analyze paint coatings on metal substrates. The characteristic parameters extracted from acquired thermal responses were compared to the results given by the classical Eddy current technique. Results obtained on samples with paint thickness varying between 60 μm and 130 μm and between 5 μm and 15 μm demonstrate that the infrared thermography allows an accurate evaluation of the heterogeneity of paint coating, whatever the thickness range.

## 2. Materials and methods

### 2.1. Numerical simulation of thermal response of paint coating samples

The main focus of the numerical simulation is to understand the effects of the thickness variation of both paint coating and substrate with respect to thermal behavior during heating and cooling process. For this reason, we suppose a simplified model: uniform and isotropic paint coatings deposited on metal substrate to avoid the direction dependent thermal conductivity; constant emissivity of the coating to ensure a good estimate of the desired temperature through the use of the equation of the infrared thermography; temperature of the sample near to that of the environment to avoid parasitic reflections; the transmission coefficient of the atmosphere close to unity and the distance between the sample, constant thermal properties of materials (thermal conductivity, heat capacity at constant pressure, etc.).

The fundamental equation of thermography of the radiance is defined as in (Eq. (1)) [28]:

$$R_{CAM} = \tau_{atm}\varepsilon R_{obj} + \tau_{atm}(1-\varepsilon)R_{env} + (1-\tau_{atm})R_{atm} \tag{1}$$

where

$R_{CAM}$: Radiance measured by the infrared camera
$\tau_{atm}$: Radiance of the atmosphere, supposed constant
$\varepsilon$: Object emissivity (in the case, the object is considered opaque)
$R_{obj}$: Radiance from the surface of the object
$R_{atm}$: Radiance of the surrounding environment considered as a black body
$\tau_{atm}$: Transmission coefficient of the atmosphere in the spectral window of interest.

Eq. (1) permits to model the thermal behavior of any type of sample. Considering an emissivity value of the coating around 0.95 as for the matt black painting used thereafter, the excitation can be assumed as being fully absorbed at the sample surface due to the high absorption coefficient of the coating layer at the excitation wavelength. With the hypothesis above, the heat convection and radiation of both coating and substrate layers can be neglected. Since, the coating thickness is very small, around few micrometers, the substrates dominated the heat conduction response and the convecto-radiative losses on the lateral sides of the sample can be neglected [29]. Thus, the equation above can be simplified as following (Eq. (2)):

$$R_{CAM} \approx R_{obj} \tag{2}$$

Regarding the thermos-physical modeling, we have opted for a very simplistic model according to the different considered assumptions. Thermo-physical properties considered in the theoretical study are then considered constant in all space directions (isotropic thermos-physical properties) and also when temperature vary.

In order to identify optimal excitation parameters, this thermal model was implemented in COMSOL Multiphysics 5.0 software. "Heat Transfer" and "Transient Analysis" modules were used to investigate the heating and cooling behavior of coating samples [30]. The 3D bi-layer geometry (Fig. 1) of a uniform and isotropic

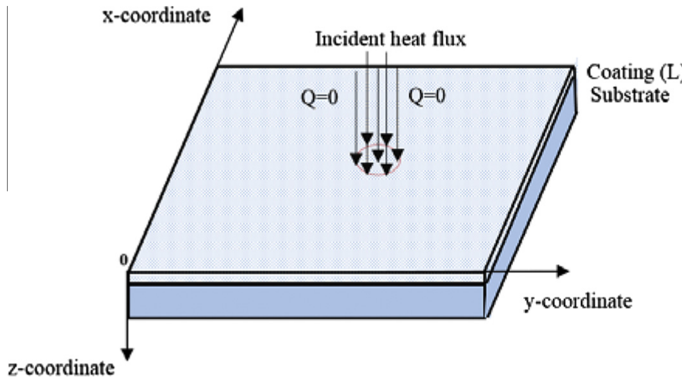


**Fig. 1.** Representative schematic of simulated bilayer model using COMSOL Multiphysics software.

paint coating deposited on a substrate was created. It includes a circular cavity as a localization of the excited areas.

Fig. 2a shows the geometry of the simulation model, based on the material and structure explained in Fig. 1. The excitation was modeled as heat flux with a finite, uniform and constant quantity of energy limited in the radial direction. Low surface heat flux 3.6 W was used in both experiment and simulation to avoid the thermal damage of paint coating by laser excitation.

Only the excited zone, as shown in Fig. 2a was finely meshed using tetrahedral grid elements to ensure the simulation accuracy and the computation efficiency [30]. In this simulation, several assumptions were made: all surfaces boundary is insulated except for the top, which faces the paint coating layer; the initial temperature is of 293.15 K; the surface is irradiated by a Gaussian excitation radiation at the top of the surface boundary; the heat flux is kept equal on the two sides of the paint coating/substrate interface.

The iterative solver used by this program can handle the complex calculations needed to solve the transient conduction heat equations in three dimensions. Furthermore, the effects of internal convection within bi-layered model of such small volume (irradiated zone) would produce a negligible impact on the overall predicted heating behavior. For these reasons and based on the hypothesis above, only heat conduction was considered in this models.

Fig. 2b shows the simulated 3D temperature field for a particular time allowing to estimate the transient state of the heating process. The time-dependent thermal response is carried out on the front side of the sample and is computed only for a part of the sample, i.e. in the center of the heated region (Fig. 2c). This thermal response reflects the thermal properties of all sample layers [31].

To analyze the influence of the paint coating variations on the thermal response and the influence of the heating source, characteristic parameters of thermal responses should be identified. The two following parameters of thermal responses were considered in this study (Fig. 2c):

- $T_{max}$: the maximum of the acquired temperature in the center of the heated zone;
- $\Delta t$: the time gap leading to 25% of temperature reduction from the maximal thermal excursion in the cooling phase.

According to heating duration, substrate thickness variations, and coating thickness, the behavior of $T_{max}$ and $\Delta t$ are observed and discussed in the application section.

### 2.2. Samples

The samples considered in this study are composed by a steel substrate with 2 mm thickness coated with black epoxy paint layer. The coating layer presents a high level of temperature resistance (more than 100 °C). Two samples with paint thickness varying between 60 μm and 130 μm and two with paint thickness in the range of 5–15 μm. The deposition is performed using a professional air spray system. Black coating color is chosen to enhance absorption along the radiance and reduce spurious reflected incident radiance for the camera [32].

The properties of the sample's layers that are analyzed with the experimental test bench, i.e. the paint coating and the steel substrate, are indicated in Table 1. These choices, which are consistent with the values shared by classical paintings and steel substrates, have been used for all the simulations.

### 2.3. Experimental setup

Experimental test bench consists of an infrared camera, a laser source and a video acquisition unit for analyzing the acquired

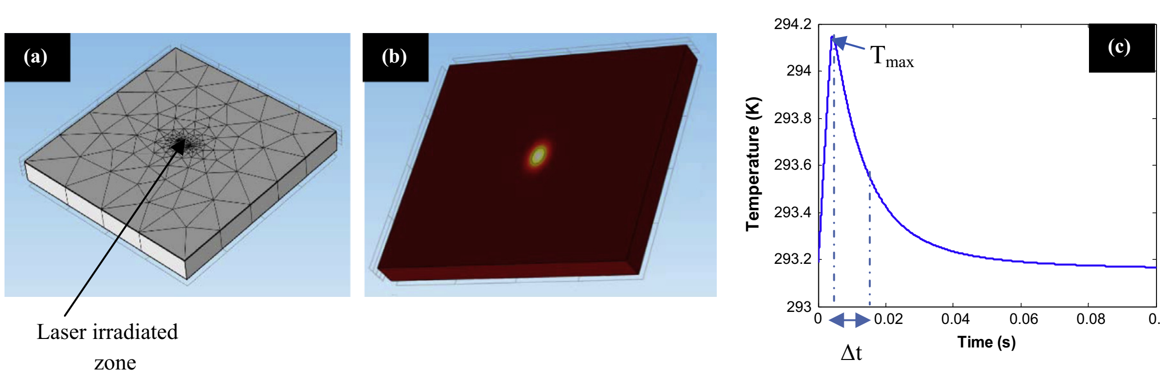


**Fig. 2.** (a) Finite-element mesh for the coated sample with hot spot for laser excitation, (b) simulated 3D temperature field at $t$ = 0.489 s and (c) time-dependent thermal response in the center of the heated zone on the front side of the sample.

**Table 1**
Thermal and physical properties of sample's layers.

| Layer (material) | Density $\rho$ (kg m$^{-3}$) | Specific heat capacity $C_p$ at constant pressure (J kg$^{-1}$ K$^{-1}$) | Thermal conductivity (W m$^{-1}$ K$^{-1}$) | Emissivity (unitless) |
|---|---|---|---|---|
| Coating (paint) | 1200 | 1000 | 0.2 | 0.95 |
| Steel | 7850 | 475 | 44.5 | 0.85 |

W = Watt, K = Kelvin, m = meter, kg = kilogram, J = Joule.

infrared thermal images [33]. The technique applied here is the pulsed Infrared thermography under laser irradiation as shown in Fig. 3.

The sample surface is heated by a laser diode with a beam power of 3.6 W/pulse and a wavelength of 808 nm. The pulse excitation of duration "$\tau$" of the laser beam is driven by a LabviewTM program. The laser diode is associated with optics of collimation and focusing in the aim to improve the convergence of laser beam and have a homogeneous power and constant radiation intensity at the front of the surface. The excitation is modulated by the controller display for power stability control of laser beam. A reproducibility test shown the stability of the signal excitation output.

An A20 FLIR SystemsTM "long waves" infrared camera has been selected for its good ratio price/performance [34]. This camera uses a focal plane array uncooled micro-bolometer detectors records the infrared thermal images (associated with an optic 45° Wide angle (45° $\times$ 34°/0.1 m)). Its NETD equals about 100 mK. The major technical specifications of the camera are: 0.1 K thermal sensitivity, 7.5–13 µm spectral range, and 160 $\times$ 120 pixels of image size. The camera has been used with a macro objective (9.2 mm) to reach a small spatial target and hence to obtain sufficient spatial resolution. In the wavelength intervals in which the infrared camera works, the spectral emissivity of the samples can be considered constant.

This camera is placed above the sample. The distance between them is 30 cm. Because of the infrared camera position, the laser beam strikes the sample perpendicularly. The shape of the laser spot is slightly elliptic. We note that the temperatures have to be measured only once and that the FLIR camera is factory-calibrated. The acquisition by the camera is synchronized with the triggering of the laser signal [35]. The experimental device was calibrated also spatially, one pixel representing 100 µm on the sample. The collimated laser spot has a diameter of about 2 mm. The spot size has a diameter of about 100 µm, which is 20 times smaller than the excitation spot size. Assuming that the temperature at the center of irradiated zone varies during a short time, a one-dimensional conduction heat transfer can be admitted, equivalent to the simplified model above. Thus the excitation can be considered punctual and the thermal analysis of our study is unidirectional. A repeatability test shown that the average error of the maximal temperature measured with the proposed experimental test bench is about 3%, while that related with the time gap insignificant.

For one acquisition point, the infrared camera provides a spatiotemporal collection of images called thermogram with a sampling frequency of 50 Hz. After the thermogram record ended in an acquisition point, the same procedure is repeated in another position. This system provides quick response, non-contact measurement of the sample surface temperature through the laser pulse.

### 2.4. Data acquisition

The thermogram recorded at one acquisition point of the sample, as shown in Fig. 4a, can be modeled by a 3D data. This data cube is constructed by stacking up the temporal sequences of thermal images [36].

Theoretically, by heating the sample with the laser having the characteristics listed above, only one point of the analyzed sample should present a thermal variation. Practically, after passing through the mirror in the deviation device, a heat dispersion is generated on the surface of the sample. With the considered spatial resolution, the thickness of real samples can be assumed homogeneous around the impact point. As a consequence, each thermal image of the spatiotemporal collection has a Gaussian distribution as shown in Fig. 4b. For this reason, the highest temperature point should be precisely estimated. In this study, we chose $X$–$Y$ the coordinates in the thermal image sequences in which the maximum temperature is reached in the thermal images sequence [31]. Once the chosen coordinates, we are able to extract the thermal response of the sample analyzed as a function of time. We have also tested rectangular and circular regions of 3 $\times$ 3 and 5 $\times$ 5 pixels around the coordinates of the hottest point. However, averaging the temperatures in this windows gives no improvement in detection of paint thickness heterogeneity and in result's quality. This results can be explained by the Gaussian distribution which is given mainly by the heat dispersion on the mirror.

The 50 Hz low sampling frequency is one of material and financial constraints of our industrial application. However, with this low sampling frequency, a precise determination of temperature attributes can be missed out. An interpolation of time-dependent thermal response is required in order to better estimate the maximum of the acquired temperature $T_{\max}$ and especially the time gap $\Delta t$. Although simple algorithms such as linear or piecewise cubic interpolation, nearest neighbor, can improve the resolution and preserve the characteristics of acquired of thermogram [37], a precise description of temperature behavior can be obtained by using a spline approach. The spline interpolation algorithm was

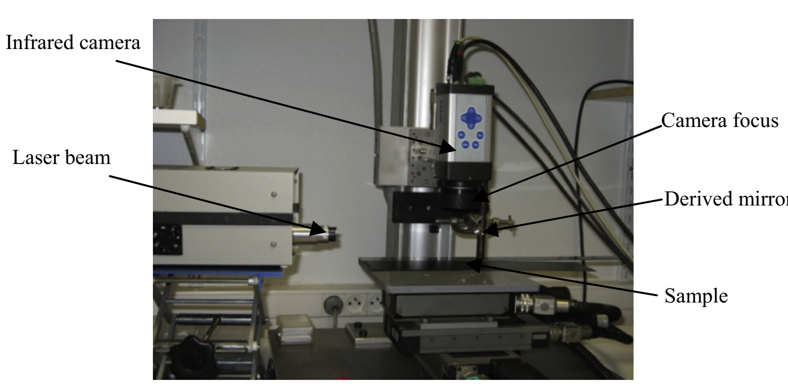


**Fig. 3.** Experimental test bench of pulsed thermography inspection.

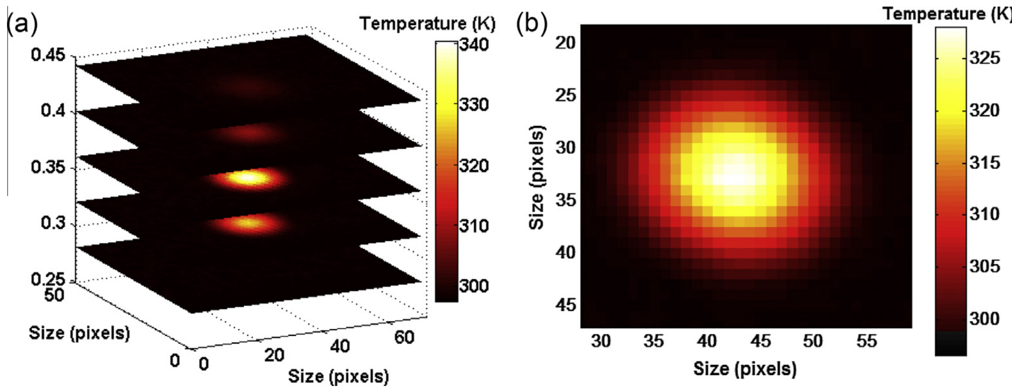


**Fig. 4.** A recorded thermogram: (a) representation of 3D data corresponding to the spatiotemporal collection of thermal images for an acquisition point and (b) the thermal image recorded at the maximum heat.

thus used in this study for the temporal re-sampling of the temperatures recorded by the infrared camera at the selected *X*–*Y* coordinate [38]. This approach produces a smoothness solution of interpolation problem with a higher resolution than the sampling rate of infrared camera [39]. Fig. 5 shows the temporal variation of the temperatures recorded by the infrared camera on which is performed the spline interpolation method with an interpolation factor of 15. The interpolated temporal variations of the temperatures allow a better estimation of the maximum temperature $T_{max}$ and implicitly of the time gap $\Delta t$.

## 3. Results and discussion

### 3.1. Numerical simulation results

Through numerical thermal response as shown in Fig. 2c, the thermal behaviors of the two parameters $T_{max}$ and $\Delta t$ were investigated with respect to the variations of the paint coating and substrate.

Fig. 6a and b shows the plot of thermal behavior tracked with theses parameters with respect to the paint coating thickness variation using excitation duration of 20 ms and steel substrate thickness of 2 mm. These figures demonstrate the relevance of these parameters to track coating thickness variation in a wide range interval [5 μm 110 μm].

It is interesting to see that a minimum value depending on the coating thickness is obtained, the temporal variations of $\Delta t$ being splitted into two regions. On the right, as expected, this parameter is directly proportional with the coating thicknesses. On the left, the $\Delta t$ parameter is inversely proportional with the coating thicknesses. This behavior can be explained by the fact that when the thickness of the paint decreases, the coating absorbs less heat the rest being led directly to the substrate layer. Under the effect of the insulation, the heat is less quickly evacuated, which is slowing the cooling time and hence increasing the $\Delta t$ parameter.

The numerical study was then performed to optimizing the thermal excitation duration. The aim is to increase the discriminative slope to paint thickness variation in the two identified domains. With the resulted optimal conditions, the influence of substrate thickness on paint thickness evaluation is investigated.

### 3.2. Numerical optimization of thermal excitation duration

To highlight only the thermal influence of thickness variations of paint coating layer, the following two steps methodology was used.

Firstly, numerical simulations were performed by varying simultaneously the thickness of the painting layer ($L$) and the pulse heating duration ($\tau$) in order to study their effects on the thermal response [31]. Fig. 7 presents the values of the $T_{max}$ parameter for paint coating thicknesses varying in the range 5–110 μm for pulse excitation of duration respectively of 4, 10, 20, and 60 ms. We can observe that this parameter is sensitive to the paint coating thickness for excitation pulse above 10 ms. As expected, a longer excitation allows a better discrimination of the coating thicknesses. However, it should be noted that a longer heating may lead to surface damage in real applications, especially when the heat dispersion of the laser is smaller.

The $T_{max}$ and $\Delta t$ evolution obtained for coating thickness in the range 5–110 μm by varying the pulse excitation duration as previously is illustrated in Fig. 7a and Fig. 7b respectively.

The result indicates that the duration of the pulsed excitation is less important. The minima of these variations slightly depend on the excitation duration and there is the same slope whatever the excitation duration. This comportment depends on the heat capacity and thermal conductivity of both layers and such an analysis should be performed for the considered application. This kind of analysis might indicate the thickness at left and right around the minimum that will have the same $\Delta t$ parameter and can be very interesting for qualifying the capacity of the infrared thermography to discriminate heterogeneities of coatings. For our application, the $\Delta t$ parameter is directly proportional with the coating thicknesses for a larger wider range of the thickness when a lower pulse excitation duration is used.

Thus, according to thickness variations of paint coating layer, a joint analysis of $T_{max}$ and $\Delta t$ behavior shows that a laser pulse duration of 20 ms is optimal.

### 3.3. Numerical simulation of the impact of substrate thickness

To get an insight on the influence of the substrate into thermal process, another numerical study was performed by imposing the pulse duration of 20 ms and varying the coating thickness in the same range, 5–110 μm. Results shown in Fig. 8 demonstrate that the metal response has no effect on $T_{max}$, whatever the substrate thickness variation, and has a negligible effect on $\Delta t$ parameter.

### 3.4. Evaluation of paint coating thickness on real samples

We consider in this application the case where the coating is a commercial paint deposited with a professional air spray system on a steel substrate so that the results could be compared to those given by a classical Eddy current technique. Nevertheless, the

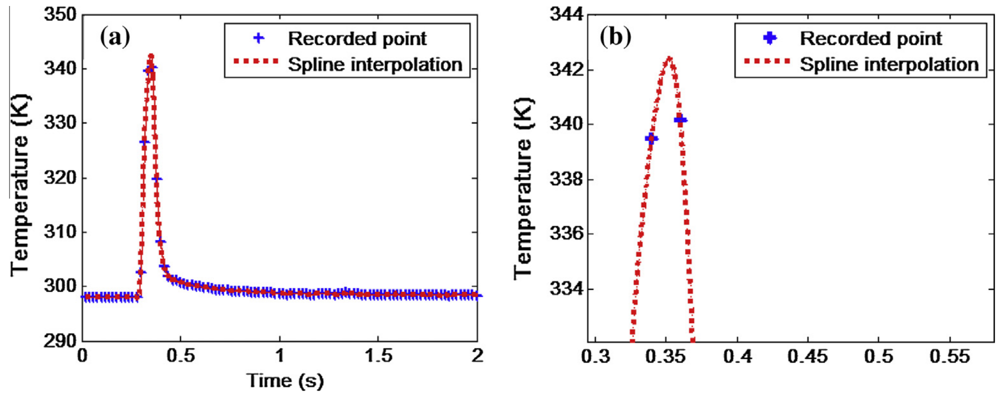


**Fig. 5.** (a) Temporal variations of the temperatures recorded by the infrared camera at the selected *X–Y* coordinate (dotted line) and temporal variations interpolated by spline (continuous line) and (b) a zoom of thermal response at excitation duration.

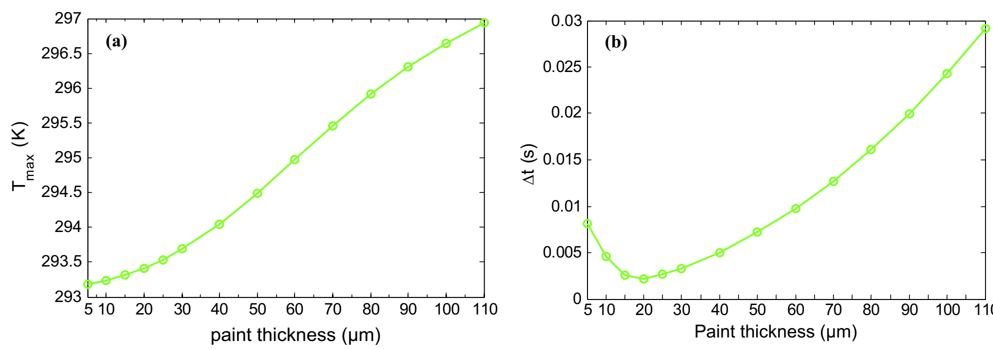


**Fig. 6.** Thermal behavior tracked by (a) $T_{max}$ and (b) $\Delta t$ parameters for an epoxy/steel sample with thicknesses of cover varying between 5 and 100 µm.

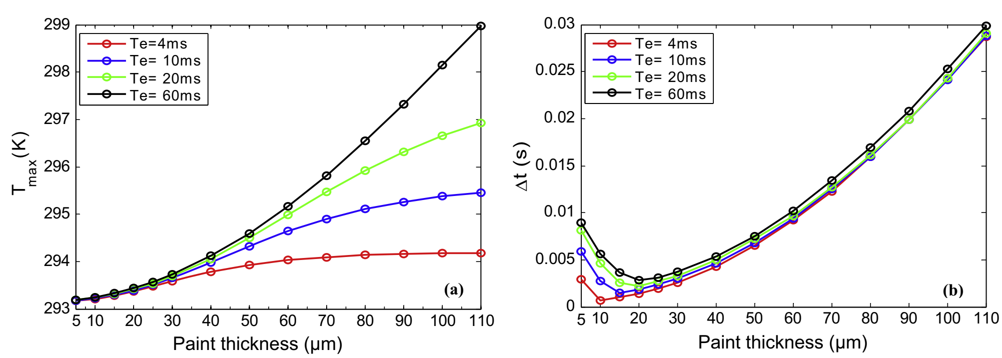


**Fig. 7.** Influence of laser pulse durations on evolution of $T_{max}$ parameter (a) and $\Delta t$ parameter (b) function of paint coating thickness. The substrate thickness was kept constant (2 mm).

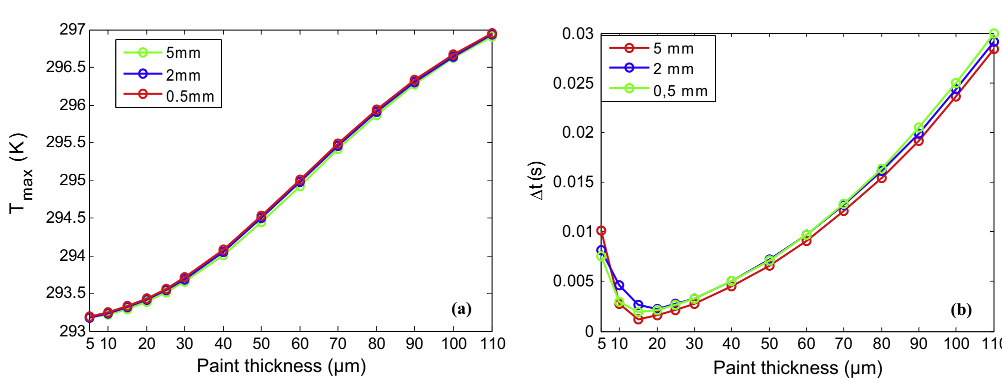


**Fig. 8.** Effect of substrate thickness 5 mm (red), 2 mm (blue), and 0.5 mm (green) on (a) $T_{max}$ parameter and (b) $\Delta t$ parameter for different paint thickness ranging between 5 µm and 110 µm. The pulse excitation duration was kept. (For interpretation of the references to color in this figure legend, the reader is referred to the web version of this article.)

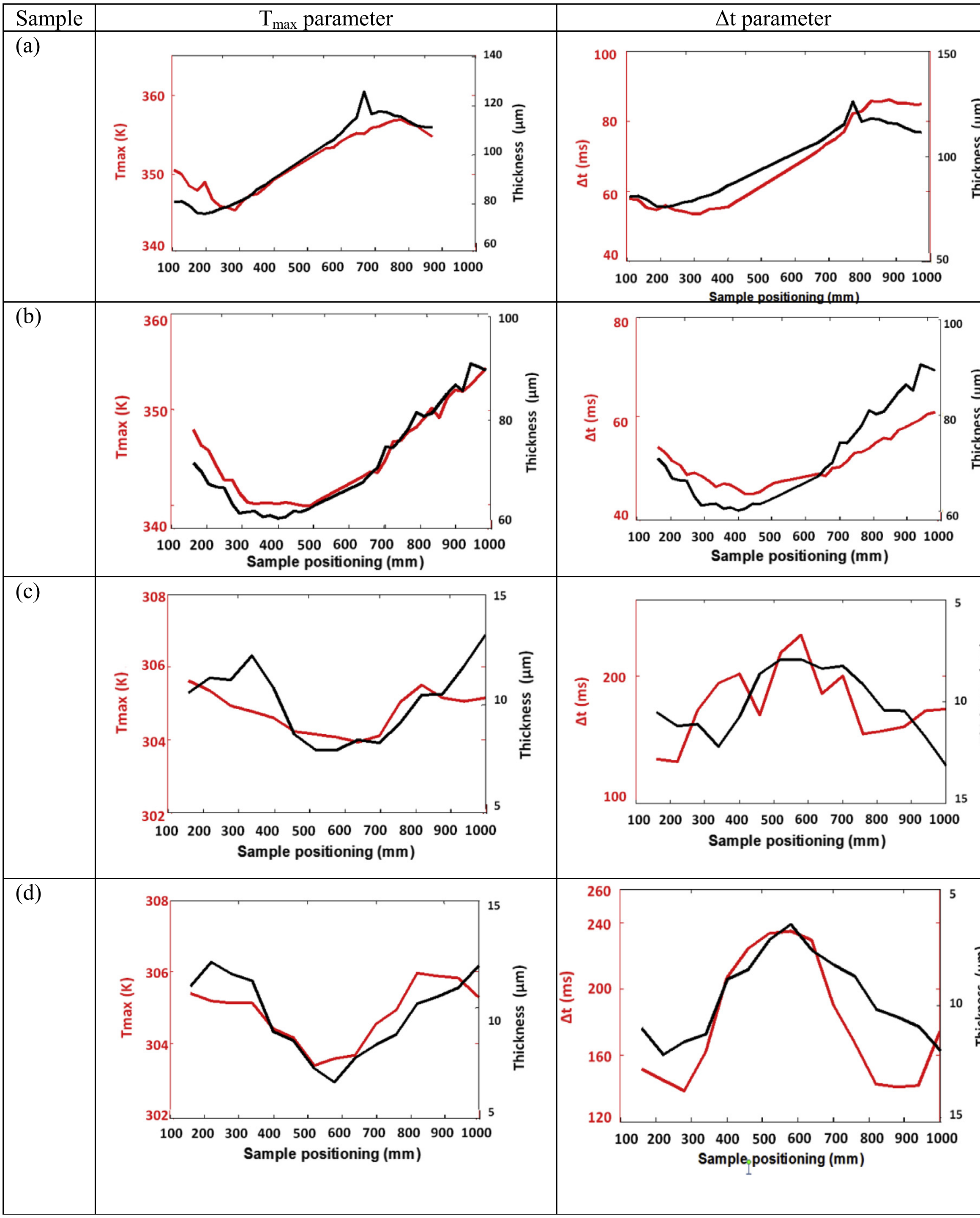


**Fig. 9.** Comparison of $T_{max}$ and $\Delta t$ parameters extracted from temporal variations of the temperatures recorded by IR camera (red curve) with the Eddy current measures (black curve) for four samples having thicknesses variations: (a) 75–130 μm. (b) 60–90 μm. (c) 7–14 μm. (d) 7–13 μm. (For interpretation of the references to color in this figure legend, the reader is referred to the web version of this article.)

presented methodology could be applied on other substrates, including nonconductive materials, and other coatings.

Accuracy of the infrared thermography laser method was compared with the Eddy current technique by measuring the thickness variations of coatings over one direction in the middle of the sample with a same spatial resolution of 15 mm. Variations of the thickness produce a modification of $T_{max}$ and $\Delta t$ parameters extracted from the thermal responses recorded in the front of the sample with the experimental test bench. The proposed methodology consists in automatically choosing the $X$–$Y$ coordinates in the thermal image sequences in which the maximum temperature is reached and interpolating the thermal responses with a spline algorithm. The interpolation factor was chosen to be 15, which is equivalent with using an infrared camera with a 750 Hz sampling rate.

Based on the numerical analysis, since the same material substrate was used with quite the same thicknesses, the change in $T_{max}$ and $\Delta t$ parameters is due to the heat conduction through the coating, which is directly related to its thickness [40].

Fig. 9 shows that the thermal response of the paint coating is very well correlated to thickness measured by the Eddy current technique. Both parameters depend on paint thickness variations. The $T_{max}$ parameter is directly proportional to the coating thickness as measured by Eddy current. The $\Delta t$ parameter change its dynamic according the range of paint thickness respectively positive for samples (a) and (b) and negatively for samples (c) and (d). This parameter is inversely proportional to the coating thickness which are lower than 15 μm. This behavior, due to transparence of the coating thickness, is in accordance with the numerical simulation results as observed in Fig. 7. We notice that the $T_{max}$ parameter is relatively high, up to 360 K, meaning that precautions should be taken for industrial applications in order to not cause damage to the coating layer. The impact of this increase in temperature during a relatively short time has to be optimized according the coating functional purpose (resistance against corrosion, aesthetic application, wear improvement, etc.).

## 4. Conclusions

This paper demonstrates that the infrared thermography is an attractive tool for the non-destructive evaluation of paint coating thickness variations. Two characteristic parameters were defined from the thermal response of coated sample. One is directly proportional with the coating thickness but practical precautions should be taken in order to not damage the coating. The second shows a minimum value depending on different factors including the heat capacity, thermal conductivity and duration of the excitation. Numerical simulations should be considered for defining optimal parameters of excitation and analyzing the behavior of these parameters.

Results obtained on paint coated samples with metal substrates show that the suggested system, using pulsed laser combined to infrared thermography, allows a good evaluation of the paint coating thickness in comparison to the Eddy current method. These results suggest the possibility and suitability of practical use of infrared thermography for evaluation of coating thickness. Although the parameter to be analyzed depend on the considered application, such technique can be successfully used to assess the heterogeneity of the coatings. It is also interesting to note that infrared thermography might be used for non-conductive substrates whereas the Eddy current method cannot be applied.

The laser, which is monochromatic and unidirectional, provides homogeneous heat, being enough sensitive to the thickness variations of paint coatings. Further studies should consider flash heating excitations to evaluate the heterogeneity of coatings for an entire sample as well as the study of samples with non-conductive substrates.

## Acknowledgment

The research for this paper was financially supported by Communauté d'agglomération de Châlons-en-Champagne, France.

## References

[1] S.C. Cha, A. Erdemir, Coating Technology for Vehicle Applications, Springer International Publishing, Switzerland, 2015, http://dx.doi.org/10.1007/978-3-319-14771-0.

[2] S. Mezghani, H. Zahouani, J. Piezanowski, Multiscale effect of paint pulverization orientation on appearance after painting, J. Phys.: Conf. Ser. 311 (1) (2011) 1–5, http://dx.doi.org/10.1088/1742-6596/311/1/012026.

[3] G. Stenberg, M. Boman, Thickness measurement of light elemental films, Diam. Relat. Mater. 5 (12) (1996) 1444–1449, http://dx.doi.org/10.1016/S0925-9635(96)00563-8.

[4] K. Chandler, R.E. Mansford, Measurement of thickness of sprayed metal coating on steel, ICE Proc. 30 (1) (1965) 131–146, http://dx.doi.org/10.1680/iicep.1965.9569.

[5] J.V. Koleske, Paint and Coating Testing Manual: 15th edition of the Gardner-Sward Handbook, ASTM International, Bridgeport, 1995. ISBN: 978-0-8031-7017-9.

[6] C.V. Dodd, W.A. Simpson, Thickness measurements using eddy-current techniques, in: Proc. Spring Conference of the American Society for Nondestructive Testing, Los Angeles, 1972.

[7] PJ. Shull, Nondestructive Evaluation: Theory, Techniques, and Applications, Marcel Dekker Ed. (2002) 848.

[8] L. Ming-Xuan, W. Xiao-Min, M. Jie, Thickness measurement of a film on a substrate by low-frequency ultrasound, Chin. Phys. Lett. 21 (5) (2004) 870, http://dx.doi.org/10.1088/0256-307X/21/5/030.

[9] D. Chen, Q. Ji, L. Zhao, H. Zhang, Application of pulsed eddy current and ultrasonic sensors in paint film thickness measuring, in: Control and Decision Conference (CCDC '09), 2009, pp. 4461–4464. http://dx.doi.org/10.1109/CCDC.2009.5192349.

[10] T. Kurabayashi, S. Yodokawa, S. Kosaka, Terahertz imaging through paint layers, in: 37th International Conference on Infrared Millimeter and Terahertz Waves, 2012, pp. 1–2. http://dx.doi.org/10.1109/IRMMW-THz.2012.6380425.

[11] K. Su, R.K. May, I.S. Gregory, P.F. Taday, Y.C. Shen, J.A. Zeitler, Terahertz sensor for non-contact thickness measurement of car paints, in: 38th International Conference on Infrared Millimeter and Terahertz Waves (IRMMW-THz), 2013, pp. 1–2. http://dx.doi.org/10.1109/IRMMW-THz.2013.6665831.

[12] Y. Izutani, M. Akagi, K. Kitagishi, Measurements of paint thickness of automobiles by using THz time-domain spectroscopy, in: 37th International Conference on Infrared Millimeter and Terahertz Waves (IRMMW-THz), 2012, pp. 1–2. http://dx.doi.org/10.1109/IRMMW-THz.2012.6380482.

[13] T. Iwata, S. Yoshioka, S. Nakamura, Y. Mizutani, T. Yasui, Prediction of the thickness of a thin paint film by applying a modified partial-least-squares-1 method to data obtained in terahertz reflectometry, J. Infrared Millimeter Terahertz Waves 34 (10) (2013) 646–659, http://dx.doi.org/10.1007/s10762-013-0015-2.

[14] M. Aoyagi, T. Hiraguri, T. Ueno, Nondestructive analysis of uneven paint coatings by dynamic heat conduction following flash heating, J. Coat. Technol. Res. 11 (3) (2014) 311–318, http://dx.doi.org/10.1007/s11998-013-9537-8.

[15] S. Bagavathiappan, B.B. Lahiri, T. Saravanan, J. Philip, T. Jayakumar, Infrared thermography for condition monitoring – a review, Infrared Phys. Technol. 60 (2003) 35–55, http://dx.doi.org/10.1016/j.infrared.2013.03.006.

[16] E. Grinzato, C. Bressan, S. Marinetti, P.G. Bison, C. Bonacina, Monitoring of the Scrovegni Chapel by IR thermography: Giotto at infrared, Infrared Phys. Technol. 43 (2002) 165–169, http://dx.doi.org/10.1016/S1350-4495(02)00136-6.

[17] M.R. Clark, D.M. McCann, M.C. Forde, Application of infrared thermography to the non-destructive testing of concrete and masonry bridges, NDT&E Int. 36 (2003) 265–275, http://dx.doi.org/10.1016/S0963-8695(02)00060-9.

[18] C. Meola, Infrared thermography for masonry structure, Infrared Phys. Technol. 49 (2007) 228–233, http://dx.doi.org/10.1016/j.infrared.2006.06.010.

[19] M.P. Luong, Fatigue limit evaluation of metals using an infrared thermographic technique, Mech. Mater. 28 (1998) 155–163, http://dx.doi.org/10.1016/S0167-6636(97)00047-1.

[20] M.L. Pastor, X. Balandraud, M. Grediac, J.L. Robert, Applying infrared thermography to study the heating of 2024-T3 aluminium specimens under fatigue loading, Infrared Phys. Technol. 51 (2008) 505–515, http://dx.doi.org/10.1016/j.infrared.2008.01.001.

[21] H. Wang, L. Jiang, P.K. Liaw, C.R. Brooks, D.L. Klastrom, Infrared temperature mapping of ULTIMET alloy during high-cycle fatigue, Metall. Mater. Trans. 31 (4) (2000) 1307–1310, http://dx.doi.org/10.1007/s11661-000-0126-y.

[22] L.D. Favro, T. Ahmed, X. Han, L. Wang, S.M. Shepard, Thermal wave imaging of aircraft structures, Rev. Prog. Quant. Non-Destruct. Eval. 14 (1995) 461–466, http://dx.doi.org/10.1007/978-1-4615-1987-4_55.

[23] M. Menaka, S. Bagavathiappan, B. Venkatraman, T. Jayakumar, B. Raj, Characterisation of adhesively bonded laminates using radiography and infrared thermal imaging techniques, Insight 48 (10) (2006) 606–612.

[24] K. Su, Y.C. Shen, J.A. Zeitler, Terahertz sensor for non-contact thickness and quality measurement of automobile paints of varying complexity, IEEE Trans. Terahertz Sci. Technol. 4 (4) (2014) 432–439, http://dx.doi.org/10.1109/TTHZ.2014.2325393.

[25] R.A. Epperly, G.E. Heberlein, L.G. Eads, A tool for reliability and safety: predictand prevent equipment failures with thermography, in: IEEE Petroleum and Chemical Industry Conference, Banff Alta, 1997, pp. 59–68. http://dx.doi.org/10.1109/PCICON.1997.648167.

[26] C. Meola, G.M. Carlomagno, Review application of infrared thermography to adhesion science, Adhes. Sci. Technol. 20 (7) (2006) 589–632, http://dx.doi.org/10.1163/156856106777412491.

[27] Q. Tang, C. Bu, Y. Liu, L. Qi, Z. Yu, A new signal processing algorithm of pulsed thermography, Infrared Phys. Technol. 68 (2015) 173–178, http://dx.doi.org/10.1016/j.infrared.2014.12.002.

[28] X.P.V. Maldague, Nondestructive Evaluation of Materials by Infrared Thermography, Springer, London, 1993.

[29] J.C. Candoré, J.L. Bodnar, V. Detalle, P. Grossel, Characterization of defects situated in a fresco by stimulated infrared thermography, Eur. Phys. J. Appl. Phys. 57 (1) (2012) 11002, http://dx.doi.org/10.1051/epjap/2011110243.

[30] J. Zhang, Y. Mizuyama, W. Xiong, Y.S. Zhou, Y.F. Lu, Simulations of heating sol–gel thin film by laser pulse train, in: Proceeding of the COMSOL Conference Boston, 2010.

[31] S. Mezghani, E. Perrin, J.L. Bodnar, J. Marthe, B. Cauwe, V. Vrabie, Evaluation of heterogeneity of paint coating on metal substrate using laser infrared

thermography and eddy current, World Acad. Sci., Eng. Technol. Int. J. Mech., Aerospace, Ind. Mech. Eng. 9 (5) (2015).

[32] T. Králík, V. Musilová, P. Hanzelka, J. Frolec, Method for measurement of emissivity and absorptivity of highly reflective surfaces from 20 K to room temperatures, Metrologia 53 (2) (2016) 743–753, http://dx.doi.org/10.1088/0026-1394/53/2/743.

[33] S. Bagavathiappan, B.B. Lahiri, T. Saravanan, J. Philip, T. Jayakumar, Infrared thermography for condition monitoring – a review, Infrared Phys. Technol. 60 (2003) 35–55, http://dx.doi.org/10.1016/j.infrared.2013.03.006.

[34] J.C. Candoré, J.L. Bodnar, V. Detalle, P. Grossel, Non-destructive testing of works of art by stimulated infrared thermography, Eur. Phys. J.: Appl. Phys. 57 (2) (2012), http://dx.doi.org/10.1051/epjap/2011110266. EDP Sciences.

[35] M.Z. Ahmad, A.A. Khan, S. Mezghani, E. Perrin, K. Mohoubi, J.L. Bodnar, V. Vrabie, Wavelet Subspace Decomposition of Thermal Infrared Images for Defect Detection in Artworks. Available from: arXiv:1508.06010.

[36] S. Mezghani, E. Perrin, J.L. Bodnar, B. Cauwe, V. Vrabie, Multiscale analysis of thermography imaging dynamic for sol–gel coating discrimination, in: 12th Quantitative InfraRed Thermography (QIRT) Conference, 2014, 199.

[37] W.C. Siu, K.W. Hung, Review of image interpolation and super-resolution, Signal & Information Processing Association Annual Summit and Conference (APSIPA ASC), 2012, 1–10, ISBN: 978-1-4673-4863-8.

[38] A. Mitra, H.S. Dhillon, Evaluating sinusoidal functions by a low complexity cubic spline interpolator with error optimization, Int. J. Electr. Comput. Energetic Electron. Commun. Eng. 1 (9) (2007) 1275–1282.

[39] K.A. Sidek, I. Khalil, Enhancement of low sampling frequency recordings for ECG biometric matching using interpolation, Comput. Meth. Programs Biomed. 109 (1) (2013) 13–25, http://dx.doi.org/10.1016/j.cmpb.2012.08.015.

[40] C.A. Decker, T.J. Mackin, Measuring film thickness using infrared imaging, Thin Solid Films 473 (2) (2005) 196–200, http://dx.doi.org/10.1016/j.tsf.2004.04.058.